Preferred citation: R. Koppolu and M. Toivakka. High-throughput processing of nanocelluloses into biodegradable barrier coatings. In *Advances in Pulp and Paper Research*, Cambridge 2022, Trans. of the XVIIth Fund. Res. Symp. Cambridge, 2022 (D. Coffin and W. Batchelor, eds), pp 217–245. FRC, Manchester, 2022. DOI: 10.15376/frc.2022.1.217

HIGH-THROUGHPUT PROCESSING OF NANOCELLULOSES INTO BIODEGRADABLE BARRIER COATINGS

Rajesh Koppolu and Martti Toivakka*

Laboratory of Natural Materials Technology, Åbo Akademi University, 20500 Turku, Finland

ABSTRACT

There is an ever-increasing interest towards utilizing nanocellulose as barrier coatings and films, with many companies moving towards pilot scale production of nanocellulose to be used primarily for barrier coatings. However, high suspension viscosity and yield stress, poor adhesion to substrates, poor moisture sensitivity, and additional drying infrastructure needed for large-scale processing of nanocelluloses are some of the challenges that need to be addressed before commercialization. The current work aims at understanding and addressing the above challenges and to develop high-throughput continuous processes required to convert nanocellulose suspensions into barrier coatings and films. Rheology of different types of nanocelluloses across a wide range of shear rates is evaluated with special attention on the influence of dispersants (carboxymethyl cellulose (CMC) and Sodium polyacrylate (NaPA)) on the suspension processability and coating quality. A slot-die applicator is used to apply nanocellulose suspensions as a thin layer on a paper substrate in a continuous process. For moisture protection, biodegradable polymers and dispersions are applied onto the nanocellulose-coated paper via

* Corresponding author

extrusion or dispersion coating. The resulting multilayer structure is then evaluated for its barrier properties viz., oxygen, water vapor, mineral oils, and grease at different test conditions. CMC addition reduces the yield stress, increases water retention, and slows down structure recovery (post high-shear) for nanocellulose suspensions, and thus has positive influence on coating quality and barrier properties. A new Casson-power-cross model was proposed to explain the viscosity behavior of cellulose nanofibrils (CNFs) across a wide shear-rate region, and Herchel-Bulkley model explains the viscosity behavior of cellulose nanocrystals (CNCs). Water vapor permeance for multilayer coatings remained below the control single-layer moisture-barrier materials, and oxygen permeance values were similar or lower than that of pure nanocellulose films. Glycerol and sorbitol plasticizers further improve oxygen barrier and kaolin addition improves the adhesion at nanocellulose/thermoplastic interface. The results provide insight into understanding the various factors that influence the continuous processing of a wide variety of nanocellulose suspensions into biodegradable barrier coatings and will pave the way for industrial production of sustainable packaging.

Key words: Nanocellulose, Roll-to-roll coating, Rheology, Barrier coatings, Multilayer coatings

INTRODUCTION

In 2018, global plastic production reached 360 million tons, out of which 40% was used for various packaging applications with the most being used only once before being discarded [1]. In addition to being non-biodegradable, common plastics are made from fossil fuels. This puts a considerable strain on both our natural resources and the environment. As countries around the world are trying to increase their plastic-packaging waste-recycling rates, there is also a shift in consumer preferences towards using more sustainable alternatives [2, 3]. Recent policy changes introduced by many economies, for example, European Union's new "Circular Economy Action Plan" [4] adopted in March 2020 is also driving the interest towards finding bio-based and bio-degradable alternatives for packaging.

One potential candidate for future packaging applications that has gained interest in recent times is nanocellulose, which is a nano-scale cellulose-based natural polymer derived from plants, fungi, and bacteria. Nanocellulose is the most researched bio-material in recent times due to its abundance, renewability, biocompatibility, biodegradability, barrier properties, and excellent functionalization

potential [5, 6]. Nanocellulose-based barrier coatings and films have attracted a lot of interest from the academia and the industry alike, due to their outstanding barrier against oxygen, grease, and mineral oils [7]. Nanocellulose is fully biodegradable, which makes it a promising bio-material to replace non-biodegradable fossil-fuel-based plastics and metallic aluminum in barrier food-packaging applications [8]. Several companies have already moved to pilot-scale production of nanocellulose to be used primarily for barrier coatings and films [9].

Depending on the fibril size, crystallinity, and synthesis route, nanocellulose is broadly classified into three types, cellulose nanofibrils (CNFs), cellulose nanocrystals (CNCs), and bacterial cellulose (BC) [5]. CNFs can be produced via mechanical defibrillation of chemical pulp [10]. However, chemical/biological pretreatments such as TEMPO-oxidation [11], periodatechlorite-oxidation [12], carboxymethylation [13], phosphorylation [14], and enzyme-mediated hydrolysis [15] are commonly used to reduce energy consumption during mechanical defibrillation and/or to improve the final properties of CNFs. CNFs have fibril diameters, lengths, and crystallinities in the range of 10 – 100 *nm*, 100 *nm* – >1 μm, and 60 – 70%, respectively [16]. CNCs are produced via strong acid (HCl, H_2SO_4, and H_3PO_4) hydrolysis of chemical pulp. They resemble rice-like structures and have lower aspect ratios compared to CNFs, and their diameters, lengths, and crystallinities are in the range of 3 – 35 *nm*, 200 – 500 *nm*, and >90%, respectively [17]. BCs are high-purity nanocelluloses produced by several species of bacteria. They have high crystallinities and tend to be longer than CNCs [18]. CNCs and CNFs are produced from wood pulp and their production processes can be scaled up which is not the case for BCs. Therefore CNCs, and CNFs are quickly becoming the preferred materials for commercial applications [16].

Despite their immense potential as barrier packaging films and coatings, there are still a few challenges that nanocelluloses face before they can be commercialized. Traditionally, nanocellulosebased films and coatings are prepared by laboratory-scale batch processes such as, solvent casting, filtration, and drawdown coating, often followed by slow drying at ambient conditions [19]. Nanocellulose suspensions have complex rheology which challenges their coating as thin uniform layers in a roll-to-roll (R2R) process [20]. For example, nanocelluloses exhibit high yield stress and viscosity, which also scale exponentially with solids concentration [21, 22]. This causes issues during pumping the suspensions and leveling off the wet coated layer. Moreover, most of the existing coating applicators are not designed to handle such high-viscosity and high-yield stress suspensions. Because of the reasons above, there is limited research on continuous coating of nanocellulose and only few research groups have demonstrated continuous roll-to-roll coating of nanocelluloses [23, 24, 25, 26, 27, 19].

Another challenge that is deterring industrial adaptation of nanocellulose for barrier coatings is that nanocellulose-based coatings are extremely moisture

sensitive, with most of the barrier properties degrading, if not disappearing completely as the relative humidity (RH) approaches 90% [28, 25]. One approach to protect nanocellulose from moisture is to have a multilayered structure consisting of nanocellulose and a moisture barrier top coating. This is already a common practice in the packaging industry where several functional layers such as, low density polyethylene (LDPE) and aluminum are coated onto paperboard to achieve the desired barrier properties [29]. By choosing a suitable biodegradable top coating, a nanocellulose-based multilayer structure can be made into a sustainable and environmentally friendly packaging material. Few researchers have demonstrated such multilayer concept by employing various bio-polymers such as guar gum, alkyd resins, polyglycolic acid, polyvinyl alcohol, polyhydroxy alkanoates (PHAs), shellac, polypyrrole, chitin, and polylactic acid (PLA) [30, 31, 32, 33, 34, 35, 36, 37, 38, 25].

The current work provides a brief overview of our research aimed at understanding and addressing the challenges that arise during high-throughput roll-to-roll processing of nanocelluloses into biodegradable single/multi-layer barrier coatings. Several nanocellulose grades ranging from pure mechanically defibrillated CNFs, CNFs produced via chemical/enzymatic pretreatments, and CNCs from acid hydrolysis were characterized for their rheological properties in the context of R2R coating. Multilayer barrier paperboards were produced by slot-die coating of nanocellulose followed by either extrusion or reverse-gravure coating of several biodegradable moisture barrier materials in roll-to-roll processes. Barrier properties of the resulting multilayer paperboards are given special attention.

MATERIALS AND METHODS

Materials

Six different nanocellulose grades were used in this work, and Table 1 lists their corresponding labels, nanocellulose type, supplier information, production method, and suspension solids content. The suspensions are labeled as nanocellulose type (CNF/CNC) followed by a letter that indicates either the production method or supplier information. For example, CNF-C is cellulose nanofibrils with carboxymethylation as pre-treatment. Several additives were used to study their impact on rheology and water retention of nanocellulose suspensions, as well as multilayer interfacial adhesion and flexibility of nanocellulose coatings. Table 2 lists the additives used in this work along with their supplier information, intended use, and addition levels. A pigmentcoated paperboard (Trayforma™ Special from Stora Enso, Finland, 205 ± 1.5 $g.m^{-2}$ and 270 ± 1.5 μm) was used as the base substrate for all the coatings and is referred to as ‘baseboard’ from hereon.

Table 1. List of nanocellulose grades used in this work

Label	*Nanocellulose type*	*Supplier*	*Production method*	*Coating solid content*[1]
CNF-M	CNF	University of Maine, U.S.A	Pure mechanical defibrillation	2.5%
CNF-C	CNF	RISE-Research Institutes of Sweden	Carboxymethylation followed by microfluidization	2%
CNF-S	CNF	SAPPI Ltd., Netherlands	Commercial grade; Pre-treatment with swelling agents followed by mechanical defibrillation	2.5%
CNF-E	CNF	Université Grenoble Alps, France	Enzymatic hydrolysis followed by defibrillation using twin-screw extrusion at 22%	12.5%
CNC-M	CNC	Melodea Ltd., Israel	Commercial grade; Sulphuric acid hydrolysis	3%
CNC-C	CNC	Celluforce Inc., Canada	Commercial grade; Sulphuric acid hydrolysis	7%

[1] Unless otherwise stated, all solids content percentages are by weight.

Nanocellulose-coated paperboards were further coated with biodegradable thermoplastics or water-based dispersions to protect the nanocellulose-coated layer from humidity. Table 3 lists these moisture barrier materials and their respective labels and coating methods. All the materials shown in Table 3 are commercial grade and their supplier information has been withheld in accordance with non-disclosure agreements. Only the main material type has been disclosed for better interpretation of results.

Suspension Characterization

Transmission Electron Microscopy and Water Retention

Transmission electron microscope (TEM) images for nanocellulose suspensions were obtained using JEOL JEM-1400 Plus (JEOL, Japan) at 80 *kV* acceleration

voltage. For TEM imaging 5 μl of 0.01% nanocellulose suspension was drop cast on carbon-coated, glow-discharged copper grids (200 mesh from TED PELLA Inc., U.S.A), and negatively stained with 1%(*w/v*) uranyl acetate. A gravimetric water retention test (Åbo Akademi type method – ÅAGWR) was performed according to TAPPI T701 pm-01. The test simulates a suspension's dewatering rate in a coating process by measuring the amount of water released from a 10 *ml* sample through a 5 μm filter membrane at a pressure drop of 0.5 *bar* during a 90 *s* time interval. The amount of water released per unit area was reported as an average from three parallel measurements.

Rheology

A modular compact rheometer, MCR 702 (Anton-Paar GmbH, Austria) was used to measure rotational, oscillatory, and thixotropic rheology parameters for the suspensions using Couette geometry (bob diameter – 26.65 *mm*, effective bob length – 40 *mm*, cup diameter – 28.93 *mm*, working gap – 5.7 *mm*) with smooth surfaces at 25 °*C*. Prior to each measurement, the samples were pre-sheared at 100 s^{-1} for 60 *s* and allowed to equilibrate for 120 *s* to remove any pre-existing heterogenities in the suspension [39]. Rotational viscosity measurements were performed in controlled shear rate mode with logarithmic shear rate ramp-up/down from 0.01 1000 – 0.01 s^{-1} (10 points/decade) with dynamic acquisition time that changes logarithmically from 60 – 1 – 60 *s* and an additional 4 *s* at 1000 s^{-1}. Data from the ramp-down curve was considered for analysis to avoid any transient viscosity effects that might show up in the ramp-up curve. Oscillatory strain sweep measurements were performed to evaluate linear viscoelastic (LVE) range and yield stress of the suspensions. Oscillatory strain was logarithmically varied from 0.01 – 100% (10 points/decade) with logarithmic decrease in acquisition time from 100 – 10 *s* at a constant angular frequency of 10 $rad.s^{-1}$. Three interval oscillatory-rotationaloscillatory test was performed to measure thixotropic behavior of the suspensions. As the name suggests, the test has three intervals, viz., 1) Rest – oscillatory mode with constant strain and angular frequency (in LVE range) of 0.1% and 10 $rad.s^{-1}$, respectively, for 60 *s* (15 points with 4 *s*/point); 2) High shear – rotational mode with constant shear rate of 1000 s^{-1} for 40 *s* (10 points with 4 *s*/point); and 3) Recovery – oscillatory mode with constant strain and angular frequency (in LVE range) of 0.1% and 10 $rad.s^{-1}$, respectively, for 120 *s* (120 points with 1 *s*/point). Time taken for the elastic modulus (G') in the recovery interval to reach 50% of the rest-interval's steady-state G' value is reported as the relative thixotropy time. Choice of the test parameters for the above rheology measurements were based on the information available in the literature and the authors' experience with measuring fiber-based nanocellulosic suspensions [40, 22, 41, 42, 43]. All the measurements were done in triplicates to ensure repeatability.

Table 2. List of additives used to study rheology and water retention of nanocellulose suspensions, as well as multilayer interfacial adhesion and flexibility of nanocellulose coatings

Additive	*Supplier*	*Intended use*	*Addition level*[1]
CMC[2] – FinnFix® 4000G	CP Kelco, Finland	Dispersant and water retention aid	2–10% (on dry nanocellulose)
NaPA[3] – Sokolan® CP10	BASF, Finland	Dispersant	2–10% (on dry nanocellulose)
Cationic starch – Raisamyl® 135	Chemigate, Finland	Adhesion at baseboard / nanocellulose interface	0.3% (primer coating)
Hyperplaty Kaolin – Barrisurf™ HX	Imerys, U.K	Adhesion at nanocellulose / extrusion-polymer interface	10, 40% (blended into CNF-M)
Glycerol	Sigma Aldrich, Finland	Plasticizer for CNF-C	2, 10% (on dry CNF-C)
Sorbitol	Sigma Aldrich, Finland	Plasticizer for CNC	20% (on dry CNC-M and CNC-C)

[1] Unless otherwise stated, all solids content percentages are by weight; [2] Carboxy methyl-cellulose; [3] Sodium polyacrylate.

Table 3. Moisture barrier materials used to protect nanocellulose-based coatings from humidity

Label	*Material type*	*Category*	*Coating method*
TP1	Low density polyethylene (LDPE)	Thermoplastic	Hot-melt extrusion
TP2	Polylactic acid (PLA)	Thermoplastic	Hot-melt extrusion
TP3	PLA, Polybutylene adipate terephthalate (PBAT) blend	Thermoplastic	Hot-melt extrusion
TP4	Polybutylene succinate (PBS)	Thermoplastic	Hot-melt extrusion
WD1	Pigment, latex (biodegradable) blend	Water-based dispersion	Reverse gravure
WD2	PLA	Water-based dispersion	Reverse gravure
WD3	Polyhydroxyalkanoate (PHA)	Water-based dispersion	Reverse gravure

Roll-to-roll Coating

The baseboard was first pre-coated with a 0.3% cationic starch primer to improve the adhesion with nanocellulose layer. Pre-coating was carried out using a laboratory-scale mini-pilot roll-to-roll coater (Rotary Koater, RK PrintCoat Instruments Ltd., U.K.) which can be fitted with different coating applicators based on the requirement. The coater has operating speeds between 1 – 50 $m.min^{-1}$, maximum drying capacity of 43 kW, and maximum coating width of 300 mm. Cationic starch coating was done using reverse-gravure coating method. The gravure roll has a surface volume of 78.5 $cc.m^{-2}$ (70 lpi x 127 μm) and applies a wet coating thickness of 16 – 25 μm (transfer fraction 0.32). Due to the low solids content of cationic starch solution (0.3%), it is difficult to accurately determine the dry thickness/coat weight of the starch-layer. Therefore, it is assumed that the coat weight of starch layer was less than 1 $g.m^{-2}$. More information about the role of substrates and primers on nanocellulose adhesion can be found in Kumar et al., [44] and Koppolu et al. [24].

The same Rotary Koater was modified in-house and fitted with a custom-built slot-die applicator to coat nanocellulose suspensions onto the starch-coated paperboard. Figure 1a shows the schematic of the slot-die coating process. Nanocellulose suspension is fed to the slot-die from a pressurized feed vessel via a gear pump. Inside the slot-die, the suspension first enters into a distribution channel (diameter 25 mm) and then passes through a narrow gap (slot-gap) before exiting the slot-die. Pressure drop across this gap results in high-shear rates which reduces the apparent viscosity of shear-thinning nanocellulose suspension. Shear rate in the slot-die is directly proportional to the flow rate (controlled by the gear pump) and inversely proportional to the square of the slot gap. Typical shear rates achieved during slot-die coating of nanocelluloses in this work are in the range of 500 – 20 000 s^{-1}. The fluidized suspension exiting the slot-die is then applied onto a moving substrate to obtain a uniform wet-coated layer. The slot-die has a coating width of 100 mm and length of the narrow slot-gap region is 50 mm. Depending on the fibril size, suspension solids content, and viscosity, slot-gap is adjusted between 500–1000 μm to avoid clogging the slot entrance. Figures 1b and c show a close-up and cross-section of the slot-die applicator, respectively. The slot-die is fixed at a 3 o'clock position with a downward offset of 5 mm against the backing roll center line (see Figure 1a), thus allowing the slot-die's top lip to function as a metering device. The advantage is that, this allows the coater's line speed to be set independent of the minimum flow rate required to achieve sufficient fluidization (low viscosity) of the nanocellulose suspension. Wet coating thickness is set by the gap between substrate and slot-die's top lip, and coating speed depends on the wet coating thickness, suspension solids, and maximum drying capacity of the coater. Table 4 lists the different nanocellulose coatings done in this work along

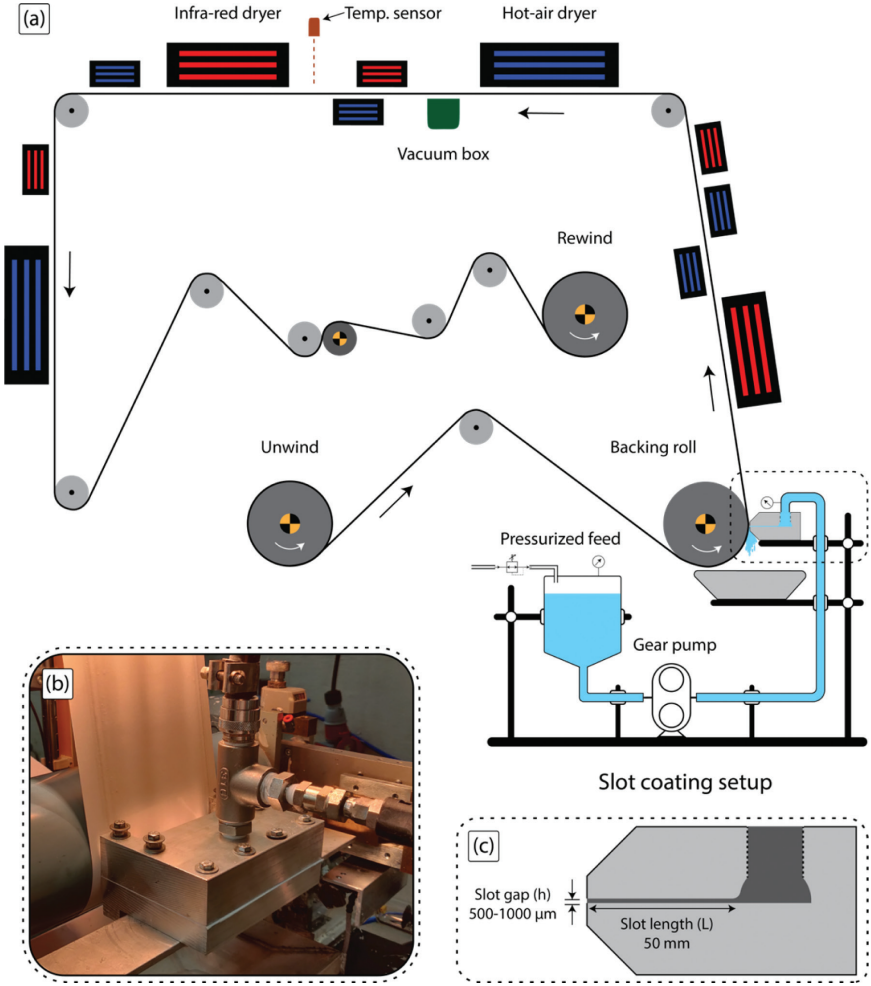

Figure 1: (a) Schematic of roll-to-roll slot-die coating of nanocellulose; (b) Slot-die coating applicator; (c) Cross-section of the slot-die

with their wet-coating thicknesses (set value), line speeds and dry-coating thicknesses (measured value).

The nanocellulose-coated paperboards were further coated with moisture-barrier materials from Table 3 to obtain multilayer-coated paperboards. Depending on the type of moisture-barrier material, two different coating methods, hot-melt

Table 4. Nanocellulose-based multilayer roll-to-roll coated samples

Nanocellulose coating (slot-die) – First layer						**Moisture barrier coating – Second layer**		
Nanocellulose	**Additives**[1]	**Wet thickness**[2] (μm)	**Dry thickness**[3] (μm)	**Suspension solids** (%)	**Line speed** ($m.min^{-1}$)	**Material**	**Dry thickness**[3] (μm)	**Line speed** ($m.min^{-1}$)
CNF-M	5 % CMC	400	8 (≈12 $g.m^{-2}$)	2.5	3	LDPE(TP1)	17	70
						PLA (TP2)	19	70
						PLA, PBAT blend (TP3)	38	70
						PBS (TP4)	22	70
						Water-based dispersion (WD1) (pigment, latex blend)	22	5
CNF-C	5 % CMC; 2, 10 % Glycerol	250x2 (double coated)	5 (≈8 $g.m^{-2}$)	2	6	LDPE(TP1)	17	70
						PLA, PBAT blend (TP3)	38	70
						PBS (TP4)	22	70
CNF-S	5 % CMC	450	8 (≈12 $g.m^{-2}$)	2.5	3	Water-based dispersion (WD2) (PLA-based)	12	5
						Water-based dispersion (WD3) (PHA-based)	12	5
CNF-E	5 % CMC / 5 % NaPA	200	15 (≈24 $g.m^{-2}$)	12.5	4	No multilayer coating		
CNC-M	20 % Sorbitol	400	7 (≈11 $g.m^{-2}$)	3	3	LDPE(TP1)	17	70
						PLA (TP2)	19	70
CNC-C	20 % Sorbitol	300	4 (≈6 $g.m^{-2}$)	7	4	Water-based dispersion (WD1) (pigment, latex blend)	22	5

[1] All additives were added with respect to dry nanocellulose.
[2] Wet thickness is the set value during slot-die coating.
[3] Dry thickness is the measured value from SEM cross-sections, and coat weight is calculated assuming a density of 1.55 $g.cc^{-1}$ and fully dense coating

extrusion for thermoplastics and reverse-gravure coating for water-based dispersions were used. Extrusion coating was done using a pilot-scale extrusion coater at Tampere University, Finland. Coating speed was set at 70 $m.min^{-1}$ and coating thickness was chosen according to manufacturer's recommendation for each material type.

Prior to extrusion coating, nanocellulose-coated paperboards were corona treated (inline) to improve the adhesion between nanocellulose and thermoplastic layers. Reverse gravure coating for water-based dispersions was done using the same Rotary Koater above at 5 $m.min^{-1}$ with the same gravure roll used for cationic starch primer coatings. Table 4 lists the moisture-barrier top coatings done on different nanocellulose-coated paperboards along with their respective measured dry-coating thicknesses.

Characterization of Coated Samples

All the coated paperboards were calendered at 100 $kN.m^{-1}$ and 60 $°C$ using a laboratory-scale soft-nip calender (DT Paper Science, Finland), and conditioned at 23 $°C$ and 50% RH for at least 24 hours before characterization. Cross-section images for the coated samples were obtained using a field-emission scanning electron microscope (FE-SEM) (LEO Gemini 1530, Carl Zeiss, Germany). Coating thicknesses for each layer were obtained from the cross-section images and the corresponding coat weights were calculated using respective material's density. Air permeability of the coatings was measured using an Air Permeance Tester (L&W, Sweden) with a measurement range of 0.003 – 100 $\mu m.Pa^{-1}.s^{-1}$. Water vapor permeance (WVP) was determined according to ASTM E96/E96M-05 at two different conditions, 23 °C/50% RH and 38 °C/90% RH, and an average from three parallel measurements is reported as $g.m^{-2}.day^{-1}.kPa^{-1}$. Oxygen permeance (OP) was measured according to ASTM F1927-07 (coulometric detector) or ASTM F3136-15 (dynamic accumulation method) at 23 $°C$ / 50% RH. F3136 is a relatively fast method to determine oxygen barrier for medium to low barrier materials, while F1927 is more sensitive to defects and is used for high oxygen-barrier materials. OpTech-O2 Model P (Mocon, U.S.A) is based on F3136 and was first used to screen out low oxygen-barrier samples. Ox-Tran 2/21 MH/SS (Mocon, U.S.A) is based on F1927 and was later used for high oxygen-barrier samples. OP of commercial cellophane measured with both the test methods/instruments gave the same value. OP from two parallel measurements is reported as $cc.m^{-2}.day^{-1}.bar^{-1}$. Grease barrier was determined according to ASTM F119-82 using olive oil at 40 $°C$. The time taken for first traces of oil to appear on the bottom side of the sample (from three parallel measurements) is reported in hours. In the interest of time, the test was ended after 500 hours. Mineral oil barrier (Heptane vapor transmission rate – HVTR) of the coated

paperboards was measured according to the method suggested by Miettinen et al. [45]. HVTR from three parallel measurements is reported as $g.m^{-2}.day^{-1}$.

Adhesion at the nanocellulose/extrusion-polymer interface was quantified by measuring the force required to peel off the top thermoplastic coating from the multilayer paperboard using SP-2000 Peel Tester (IMASS, U.S.A.). A tape (TZe-C51, Brother, U.K.) was attached to the surface of the substrate at one edge while the opposite edge was attached to a clamp, which in turn was connected to a 50 *N* load cell. The tape was pulled over a length of 26 *mm* at a speed of 5 $mm.s^{-1}$, and the force required to peel the tape was measured by the load cell. Average peak force from five parallel measurements was reported in *N*. This test was done for CNF-M + extrusion coated samples to study the influence of mineral pigment addition on adhesion with thermoplastics.

RESULTS AND DISCUSSION

TEM

Morphology of nanocelluloses can be considered as a spectrum that depends on the raw material source and the processing route. Figure 2 shows the TEM images of all the six nanocellulose grades from Table 1. CNF-M is produced with just mechanical defibrillation and therefore shows relatively coarse fibers compared to the rest. CNF-C and CNF-S are chemically pre-treated with carboxymethylation and swelling agents (Morpholine, Potassium Hydroxide, Calcium Thiocyanate), respectively, and followed by mechanical defibrillation. Chemical pretreatments help to delaminate cellulose fiber walls and increase electrostatic repulsion between the nanofibrils, which in turn improve the efficiency of mechanical defibrillation [16]. Therefore, CNF-C and CNF-S show much finer fiber structures than CNF-M. Enzymatic hydrolysis typically uses single-component endoglucanase-based enzymes which are known to have high specificity towards disordered (amorphous) regions of the cellulose [46]. Therefore, enzymatic hydrolysis weakens the amorphous regions of the cellulose fibers and mechanical defibrillation severs these weaker regions leaving behind smaller fibrils with a lower degree of polymerization compared to other CNF grades [47]. It can be seen form Figure 2d that CNF-E has shorter fibers that resemble CNCs but are relatively thicker. CNCs are on the finer side of the nanocellulose spectrum as acid hydrolysis removes most of the amorphous regions and only crystalline parts of the cellulose fibers remain intact. CNCs have lower yield than CNFs as the amorphous part is removed by the acid. Shorter fibers/crystals in CNF-E/CNCs might result in stiff and brittle coatings and therefore need higher amount of plasticizer to deliver their barrier properties.

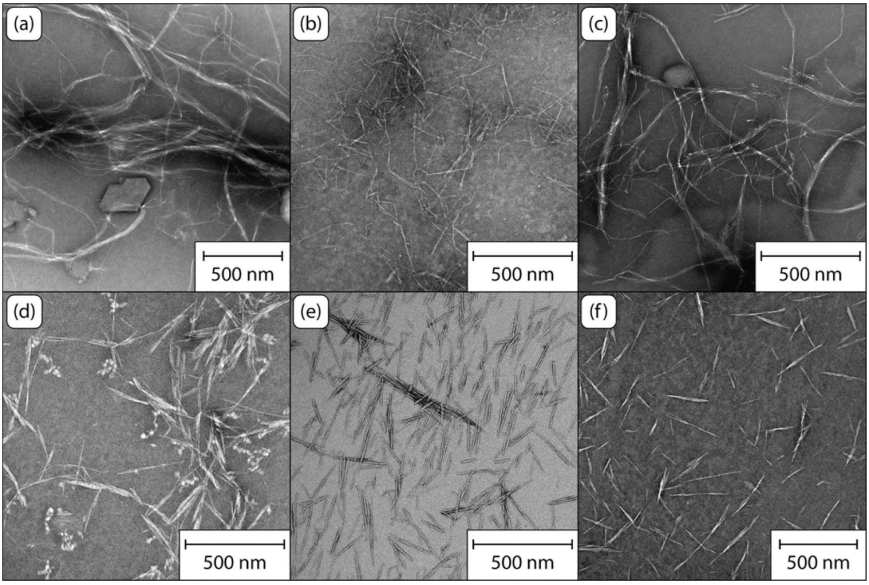

Figure 2. TEM images of (a) CNF-M, (b) CNF-C, (c) CNF-S, (d) CNF-E, (e) CNC-M, and (f) CNC-C

Rheology

Yield Stress

Nanocellulose suspensions exhibit high yield stresses due to inter-fibril hydrogen bonds and mechanical entanglement of high-aspect ratio fibers. The yield stress has been shown to scale exponentially with solids content with a power of ≈2.5 [21]. The high yield stress of nanocellulose suspensions can cause various problems in a coating process, such as cavitation during pumping due to increased resistance to flow, non-yielding regions within the coating head leading to coating defects [48], and compromised barrier properties from the inability of the nanocellulose layer to reorganize itself into a tightly packed structure. One common method to evaluate yield stress of a suspension is by performing an oscillatory amplitude sweep measurement at a constant angular frequency, evaluate the yield stress as the shear stress at the limit of the linear viscoelastic region (LVE) [43].

Figure 3a shows the yield stress values for the nanocellulose suspensions used in this work. It is evident that CMC and NaPA dispersants reduce the yield stress considerably for the CNF suspensions. CMC and NaPA are typical dispersants used in mineral pigment coating formulations to improve the colloidal stability via electro-steric stabilization [49]. The influence of various additives on rheology and

flocculation of nanocellulose suspensions has been studied in detail by Karppinen [50]. Lower yield stress and higher colloidal stability can be attributed to increased repulsion between the charged CNF fibers. CNF-M and CNF-E have yield stress measured as a function of CMC/NaPA addition levels. It can be seen that for CMC addition, yield stress reduces initially and then starts to increase again, indicating an optimum level around 5%. Higher addition levels can cause excess dispersant not adsorbing onto the fiber surfaces, which increases the ionic concentration of water phase and leads to increased flocculation as the electric double layers are compressed [49]. For NaPA, the yield stress continues to decrease with increasing addition levels. This could mean either that an optimum dispersant loading has not yet been reached or there is too much dispersant that might be creating smaller and stronger flocs that flow as individual entities. This could create an illusion of lower yield stress, but eventually results in poor coating quality (as will be demonstrated later on).

It is also be seen from Figure 3a that sorbitol addition to CNC-C reduced the yield stress. Sorbitol is a small molecule and is unlikely to cause steric stabilization of CNCs. One possible reason could be that the high addition level of sorbitol (20%) reduces the CNC to water concentration from 7.5 to 6.3%, and thereby the yield stress, which appears to be controlled by the CNC concentration rather than that of the sorbitol.

Viscosity Modeling

In a typical roll-to-roll coating process, a nanocellulose suspension experiences a wide range of shear rates that increase from rest to as high as $10^5\ s^{-1}$ (depending on the coating applicator and line speed) and back to rest in less than a second. Therefore, it is important to understand the rheological behavior of nanocellulose suspensions across the entire shear rate region. It is a well-established phenomenon that nanocellulose suspensions are highly shear thinning [42, 22]. Figure 3b shows viscosity vs. shear rate plots for four different nanocellulose grades, CNF-M, CNF-C, CNF-E, and CNC-C with suspension solids content varying from 2 – 12.5%, and all of them show shear-thinning behavior. The overall viscosity curve for CNFs can be divided into three zones, viz., low-shear, transition, and high-shear. Similar viscosity curves are reported for most of the CNF suspensions [50, 40, 42]. Despite their low solids content, CNF-M and CNF-C have viscosity values close to CNF-E and CNC-C (Figure 3b). A possible reason is that both CNF-M and CNF-C have relatively longer fibrils (Figure 2) that could cause more mechanical interlocking and therefore higher viscosities. CNC-C has viscosity close to CNF-E at low shear rates, but as the shear rate increases, the viscosity decreases significantly faster than for the CNFs. This is because, it is easier for the short and stiff cellulose nanocrystals to align in the direction of the flow compared to longer and flexible fibrils in the CNFs.

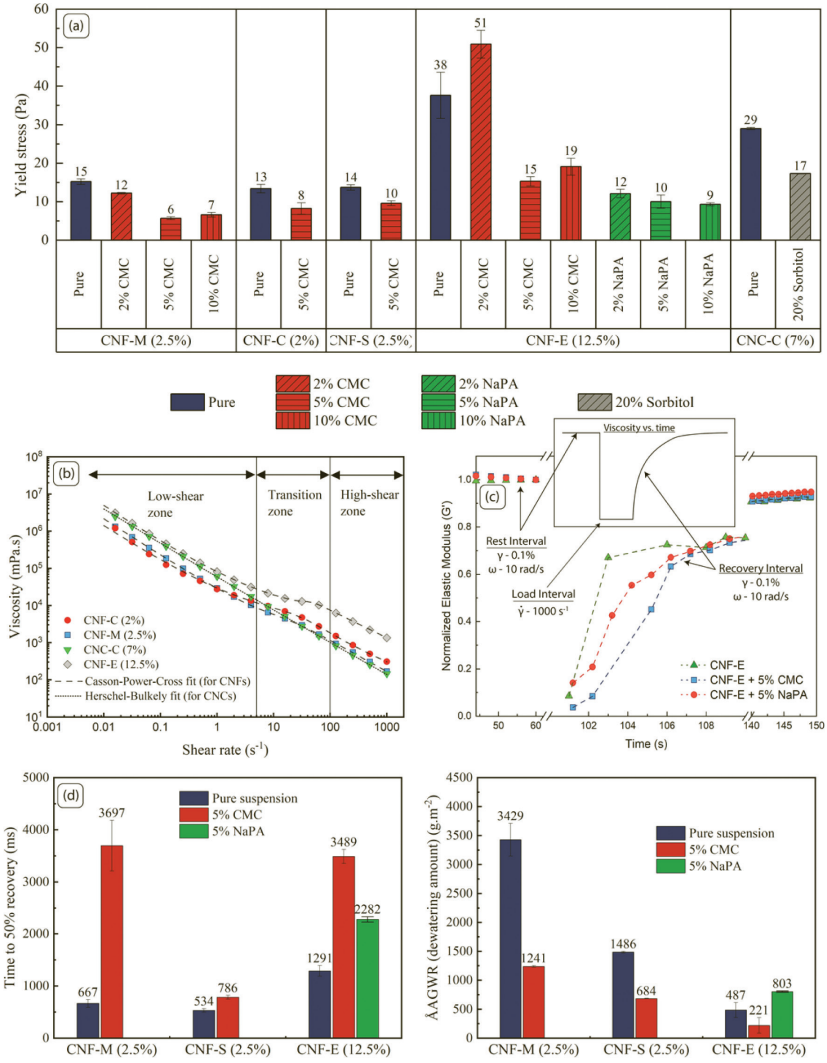

Figure 3. (a) Yield stress of nanocellulose suspensions with/without dispersants; (b) Viscosity vs. shear rate for CNF-C, CNF-M, CNF-E, and CNC-C along with their corresponding curve fits; (c) Normalized elastic modulus vs. time for rest and recovery intervals from a 3-Interval thixotropy test for CNF-E with 5% CMC/NaPA addition (insert shows a depiction of viscosity vs. time curve for this type of test); (d) Time taken for elastic modulus to recover to 50% of rest interval's steady state value for CNF-M, CNF-S, and CNF-E with/without dispersant addition; (e) ÅAGWR for CNF-M, CNF-S, and CNF-E with/without dispersants

Several rheology models have been proposed in the literature to describe shear-thinning behavior of nanocellulose suspensions, and are briefly summarized in the review article by Li et al., [42]. However, these rheology models have certain shortcomings. For example, they fit the viscosity data only in a certain shear-rate range, or require evaluation of additional parameters such as volume fraction and aspect ratio of the fibrils that can be difficult to determine accurately. The complex behavior of CNF suspensions makes it challenging to use traditional rheology models to accurately explain their behavior across a wide shear rate range. For example, Casson model, which is generally used to describe the behavior of yield stress suspensions [43], fits the shear-stress/shear-rate curve of CNF suspensions only at low shear rates and deviates considerably after the transition zone. Similarly, power-law model [43] fits the shear stress data at high shear rates and deviates at shear rates below the transition zone. Casson and power-law fits for shear stress data of CNF-M and CNF-E are given in the supporting information.

We propose a new Casson-power-cross rheology model (Equation 1) that fits the viscosity data across the entire shear rate range for CNFs studied herein. In the proposed model, the Casson model is used to explain the rheology-behavior in the low-shear zone and the power-law model for high-shear zone. λ (in Equation 1) has the unit of time and its inverse gives the inflection shear rate at which transition from Casson to power-law occurs. It can be seen from Figure 3b that the proposed Casson-power-cross model fits the viscosity data quite well ($R^2 \approx 0.99$) across the entire shear-rate range for CNF-C, CNF-M, and CNF-E suspensions that span across a wide range of solids content. The model also agrees with viscosity data for CNF suspensions with CMC and NaPA at all addition levels. A table with Casson-power-cross fit parameters for CNFs used in this work is given in the supporting information. Yield stresses obtained from the model are close to those obtained from above amplitude sweep measurements. Power-law indices for pure CNF suspensions in the high-shear zone varied from 0.18 to 0.39, and their inflection shear rates from 10 to 58 s^{-1}. This Casson-power-cross model can be useful for computational fluid dynamics when designing and optimizing new coating applicators for nanocellulosic materials. Also, with the fit, one can obtain useful characteristic parameters (yield stress, transition shear rate, high shear rate shear thinning power law index) with just one flow curve. An indepth understanding on the correlation between CNFs' physical properties and variables from Casson-power-cross model requires additional suspension characterization and significant time resources, and therefore, goes beyond the scope of this work. Future studies will explore this topic in more detail. CNCs do not have the transition zone and a yield stress-based power-law model such as Herschel-Bulkley (Equation 2) [43] fits the data very well (Figure 3b).HerschelBulkley fit parameters for CNCs are given in the supporting information.

$$\text{Casson-power-cross model: } \tau = \frac{(\sqrt{\tau_y} + \sqrt{\eta_p \dot{\gamma}})^2 - k\dot{\gamma}^n}{1 + (\lambda\dot{\gamma})^m} + k\dot{\gamma}^n \quad (1)$$

$$\text{Herschel-Bulkley model: } \tau = \tau_y + k\dot{\gamma}^n \quad (2)$$

τ, τ_y, η_p, k, n, λ, m, and $\dot{\gamma}$ are shear stress, yield stress, plastic viscosity (casson constant), consistency index, power-law index, relaxation time, cross exponent, and shear rate respectively.

Thixotropy and water retention

Once nanocellulose suspension is coated onto a paper substrate, thixotropy and water retention can be used to predict the development of coating quality as the wet suspension consolidates into a dry coated layer. As the nanocellulose suspension exits the slot-die and shear forces are completely removed, it then starts to regain its original structure and viscosity. If this recovery time is short, viscosity of the wet coated-layer increases abruptly by several orders of magnitude. This makes it harder for the wet layer to reorganize itself into a tightly packed microstructure, thus resulting in a poorly formed dry layer. Figure 3c shows normalized elastic modulus during rest and recovery intervals for CNF-E with 5% CMC and NaPA addition. It is evident that pure CNF-E suspension recovers its elastic modulus very quickly compared to that with CMC or NaPA, with CMC taking the longest time to recover its structure. Post the high-shear interval, the charged dispersants adhered on CNF fibrils slow down the structure regeneration due to electro-steric effects. This is much more pronounced for CMC due to its longer molecule chains. Figure 3d shows the time taken for elastic modulus (G') in the recovery interval to reach to 50% of rest interval's steady state value for CNF-M, -S, and –E with/without dispersants. It can be seen that for all the suspensions, CMC addition increases the recovery time and therefore could have positive impact on coating quality.

Gravimetric water retention (ÅAGWR) shows how readily a suspension dewaters during a coating process. A suspension with high water retention (slow dewatering rate) will give the wet coated layer sufficient time to reorganize itself into a uniform and tightly packed structure. Low water retention on the other hand, releases water quickly into the base substrate and immobilizes the wet coated layer rapidly, thus potentially resulting in non-uniformities and coating defects (as will be demonstrated later on). Moreover, faster water release also reduces the wet strength of the base paper leading likely to runnability issues at high speeds. It should also be noted that too high water retention might lead to slower drying times, and therefore, an optimum water retention value must be chosen to achieve

the desired coating quality without compromising much on coating speeds. Figure 3e shows the water retention values for CNF-M, CNF-S, and CNF-E with/without dispersants. CMC has cellulose as it backbone, which in itself has higher affinity to water and therefore increases water-phase viscosity of CNF suspensions. This results in an increased water retention (lower value of ÅAGWR) of a suspension. NaPA also has high affinity to water, but its influence on water-phase viscosity of CNF suspensions is not as high as that of CMC due to the former's low molecular weight. Moreover, as discussed in the yield stress subsection above, NaPA might be forming stronger and smaller CNF flocs due its possible excessive addition level. This could weaken CNFs' hydrogen-bond network with water molecules and therefore, might lead to a lower water retention (higher value of ÅAGWR). Based on the observations from yield stress, thixotropy, and water retention, it can be predicted that using 5% CMC as a dispersant should have a positive effect on CNF coating quality in a high-throughput roll-to-roll process. Without CMC addition, it was observed that coating quality of CNFs was poor and barrier properties were non-existent.

Characterization of Coated Samples

Unless specifically stated, all the roll-to-roll coated samples discussed below have 5% CMC and 20% sorbitol added to CNFs and CNCs, respectively.

Coating Structure

SEM cross-sections for the single/multi-layer roll-to-roll coated samples are shown in Figure 4. CNF-C and CNF-E represent two ends of the coating thickness (5 and 15 μm, respectively) and suspension solids content (2 and 12.5%, respectively) used in this work. All the coated nanocellulose layers show unifrom coverage of the base sheet. Air permeability of the samples was below the instrument's detection limit, which also implies full coverage. This demonstrates the suitability of slot-die applicator to handle a wide range of nanocellulose suspensions. Due to the inherent moisture sensitivity of the nanocellulose-based coatings, which deteriorates barrier properties, a polymer-based top coating was added to provide moisture protection. In addition, the top coating also helps with sealability of the packaging material during converting operations. One of the drivers for using nanocellulose for barrier coatings is its biodegradability. Keeping that in mind, biodegradable materials were chosen for moisture barrier top coatings. The multilayer paperboard can be made more sustainable if the top coating material is both bio-based and biodegradable. PLA (TP2, TP3, and WD2), PBS (TP4), and PHA (WD3) are both bio-based and biodegradable [51, 52, 53], while

PBAT (TP3) is biodegradable [54], but fossil-fuel based. Although the main constituents of WD1 are unknown, it is a commercial pigment/latex-based dispersion which is certified to be compostable. Finally, LDPE is both fossil-fuel based and non-biodegradable, and was used as reference material.

Figures 4c and d show extrusion coated TP3 and reverse gravure coated WD1 on CNF-M, respectively. It can be seen that both coating methods form uniform multilayer structure without disturbing the CNF layer underneath. A similar behavior is seen when TP2 and WD1 were coated with their respective coating methods on CNC-M and CNC-C (Figures 4e and f). Crosssection images (not shown here) of the remaining multilayer coated samples listed in Table 4 also show uniform coated structures. One of the challenges with using thermoplastics is that they might not adhere very well to the polar CNF layers. Figure 4g shows delamination occurring at CNF-M/TP4 interface, despite the corona treatment of the CNF-M-coated surface prior to extrusion coating. By blending kaolin into CNF-M, the adhesion with extrusion polymer can be improved (see Figure 4h). Influence of kaolin addition on the barrier properties and adhesion of CNF-M containing multilayer paperboard is discussed in detail in the following subsections.

Water Vapor Barrier

Figure 5a shows water vapor permeance (WVP) for single-layer nanocellulose and moisturebarrier material coatings on paperboard at two different conditions, 23 °*C* / 50% RH and 38 °*C* / 90% RH. As expected, none of the nanocellulose-based coatings show any barrier against water vapor and their WVP values are similar to that of the baseboard at both the test conditions. On the other hand, biodegradable thermoplastic and water-based dispersion-coated paperboards show over 70% reduction in WVP compared to pure nanocellulose-coated paperboard, while LDPE-coated paperboard (TP1) has the highest reduction in WVP of 90% at both conditions. Multilayer-coated paperboards show the same WVP as that of the top-coated moisture barrier layer.

Oxygen Barrier

Oxygen is a very small molecule that passes through the tiniest of gaps in the coating structure and diffuses through most moisture barrier materials [55], therefore, it is one of most challenging barrier properties to achieve. Figure 5b shows oxygen permeance values on a logarithmic scale for nanocellulose-based petridish films, single and multi-layer roll-to-roll coated samples, and also for single-layer thermoplastic and water-based dispersion coated-paperboards at 23 °*C* / 50% RH. Despite their barrier against water vapor, thermoplastic and water-based

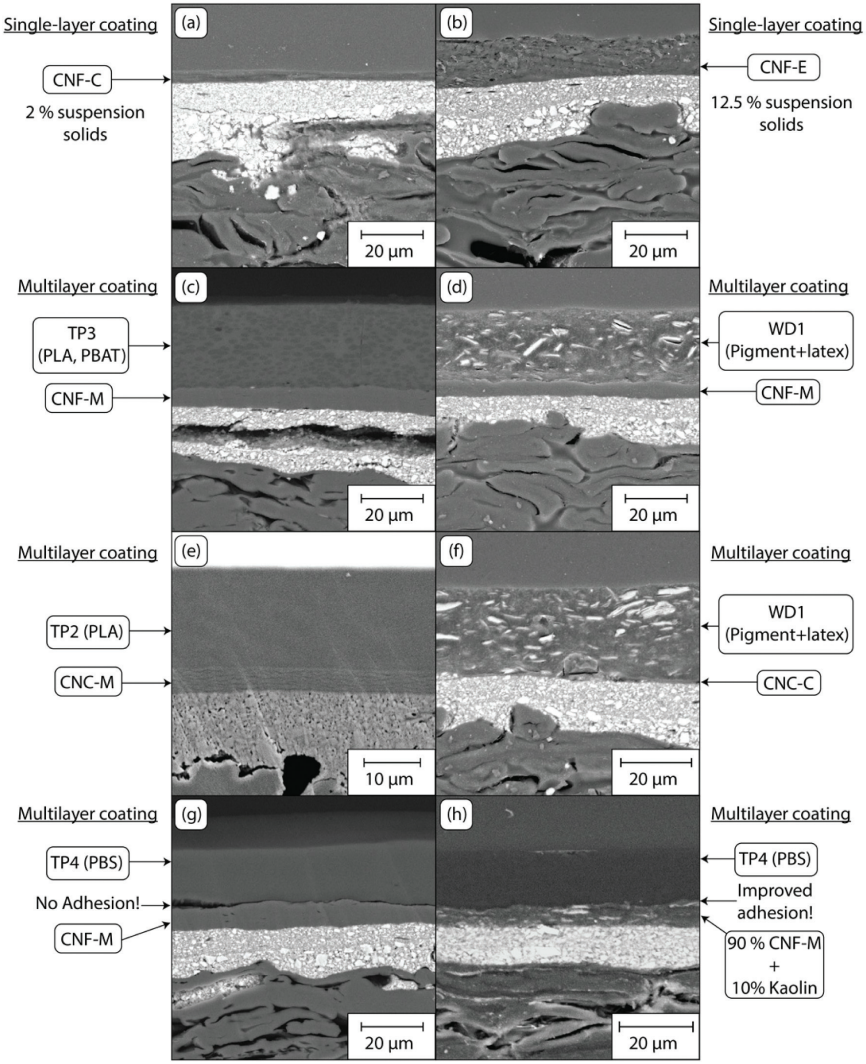

Figure 4. SEM cross-sections for different roll-to-roll coated samples

dispersion-coated paperboards show poor or no barrier against oxygen, ranging from 334 to 9428 $cc.m^{-2}.day^{-1}.bar^{-1}$. Nanocellulose films are known to exhibit excellent barrier against oxygen and the same can be observed for the CNF-based petri-dish films used in this work (Figure 5b). OP of CNF petri-dish films, which was adjusted to the corresponding R2R coating thicknesses for easier comparison

was approximately 10 $cc.m^{-2}.day^{-1}.bar^{-1}$. CNC films were brittle and reliable measurement of their oxygen permeance was not possible. Addition of sorbitol as a plasticizer produced sticky films, which could not be separated from petri dishes. Figure 5b shows that all the single layer nanocellulose-based paperboard samples have poor oxygen barrier compared to their respective petri-dish films. In a roll-to-roll process, wet nanocellulose suspension is dried very quickly under harsh conditions, where the surrounding temperatures can reach 200 °*C*. This can lead to cracks and pin-holes in the dry nanocellulose coating, which in turn will have a negative effect on oxygen barrier of the coated samples. In contrast, the slow drying and the mild self-assembly conditions used to make petri-dish films result in uniform and dense structures required for oxygen barrier.

An interesting outcome of the multilayer coating is that it seems to restore the oxygen barrier of R2R coated nanocellulose-based paperboards to the same OP as that of their corresponding petri-dish films. Both extrusion and reverse-gravure coating methods have this effect on the oxygen barrier. A possible explanation could be that during hot-melt extrusion, the molten polymer softens the nanocellulose layer sufficiently enough to seal any cracks/pinholes in the nanocellulose structure. In reverse-gravure coating, water from the dispersion could soften the nanocellulose layer which in turn helps seal the cracks/pinholes. In addition, the moisture barrier material might also plug the cracks/pinholes, and since the relative area of cracks/pinholes is very small, just sealing them could be sufficient to restore the oxygen barrier. Based on the observations from Figure 5, it can be said that multilayer coating with nanocellulose and a moisture-barrier material results in a paperboard with similar (or in some cases higher) oxygen barrier as pure nanocellulose films of equivalent thickness, while also having a high water vapor barrier. The highest OP of 2 $cc.m^{-2}.day^{-1}.bar^{-1}$ was achieved fro the CNF-s+WD3 sample.

Glycerol was added to CNF-C at 2 and 10% to study the influence of plasticizer on barrier properties. With increasing glycerol addition, OP of CNF-C-based multilayer paperboard further decreases (Figure 6a). Glycerol addition increases the flexibility of nanocellulose structure, which in turn reduces the probability of crack formation. The lowest OP value of the glycerol containing multilayer structure at 50% RH was 2.5 $cc.m^{-2}.day^{-1}.bar^{-1}$, which is similar to that of pure CNF-C films of equivalent thicknesses at 0% RH (measured value of 3.1 $cc.m^{-2}.day^{-1}.bar^{-1}$). Barrier packaging paperboard is usually formed into different shapes according to the end use, and plasticizers could play a vital role in preserving the barrier properties upon creasing and folding. Therefore, future work should clarify the role of plasticizers on OP after such converting operations.

Hyper-platy kaolin was blended into CNF-M at 10 and 40% levels to study the influence of mineral pigments on adhesion with the thermoplastic layers, and its impact on barrier properties. With increasing addition levels, pigment particles

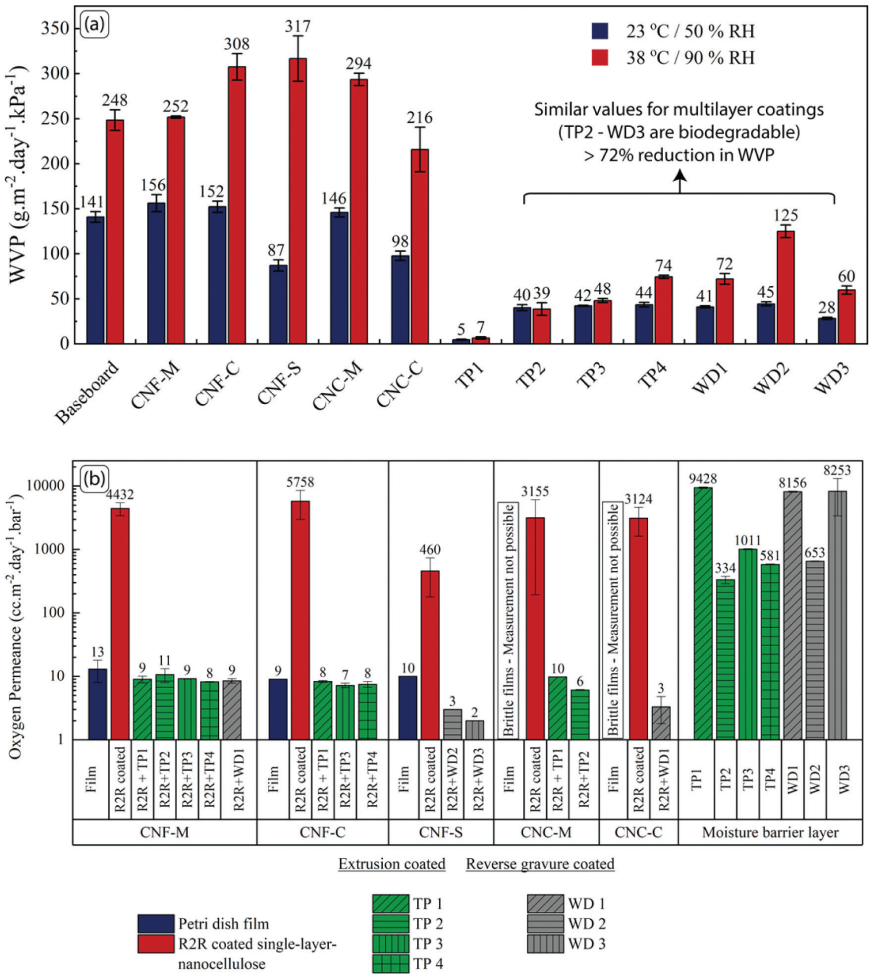

Figure 5. (a) WVP for different single-layer R2R coated paperboards at 23 °*C* / 50% RH and 38 °*C* / 90% RH; (b) OP of nanocellulose films and single/multi-layer R2R coated paperboards at 23 °*C* / 50% RH.

disturb the densely packed nanocellulose structure and therefore result in poor barrier performance. From Figure 6b, it is evident that kaolin addition increases the OP significantly. However, at a low kaolin addition level of 10%, the increase in OP is quite small and it could be suitable for applications with medium oxygen barrier requirements, provided sufficient adhesion with thermoplastic is achieved.

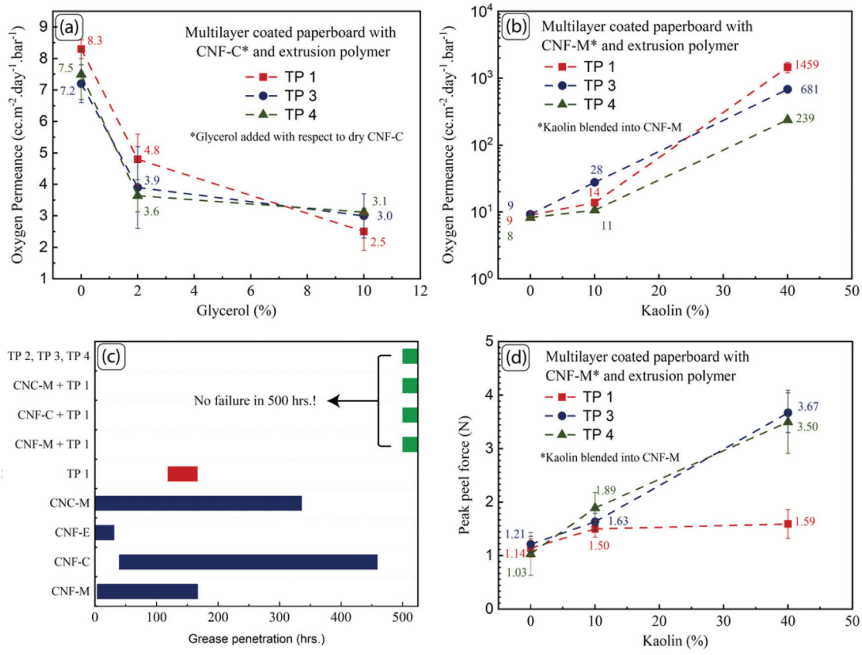

Figure 6. (a) Influence of glycerol addition on OP of multi-layer coatings with CNF-C at 23 °*C* / 50% RH; (b) Influence of kaolin addition on OP of multi-layer coatings with CNF-M at 23 °*C* / 50% RH; (c) Grease penetration time for different single/multi-layer coated paperboards. Start point of the bar indicates failure of first sample and the end point indicates failure of last of 3 parallel samples; (d) Peak adhesion force for multi-layer coated paperboard at nanocellulose/extrusion-polymer interface.

Grease and Mineral-oil Barrier

Similar to OP values, R2R coated nanocelluloses show a wide variation in grease barrier, measured with olive oil at 40 °*C*. Analogously, when coated with the moisture barrier layer on top, the grease barrier improves, showing no failures during the test period of 500 *hrs.* (Figure 6c). TP1 (LDPE) as such does not have any barrier to olive oil, but multilayer coatings based on TP1 show grease barrier due to the nanocellulose layer underneath. Other moisture barrier materials used in this work already provide grease barrier.

Most of the single layer R2R coated nanocellulose-paperboards show barrier against mineral oil (HVTR). n-Heptane was used for the test and no n-Heptane vapor escaped through the nanocellulose coated paperboard during the 48 hour test period. HVTR for these coatings is therefore not reported specifically. The

only exception is CNF-E coating with NaPA as the dispersant. For this coating, HVTR was 440 $g.m^{-2}.day^{-1}$. For comparison, baseboard has HVTR of ≈1100 $g.m^{-2}.day^{-1}$. As discussed in the rheology section above, NaPA addition to CNF-E might have created smaller flocs, and when coated, these flocs immobilize immediately due to the low water retention, which might create large enough cracks for n-Heptane vapors to pass through. Supporting information has SEM surface images of CNF-E-based coating with 5% CMC and NaPA addition. The cracks caused by NaPA are clearly visible in the images.

Adhesion at Nanocellulose/Extrusion-polymer Interface

Adhesion of extrusion polymer depends on the surface roughness, porosity, and surface energy of the substrate [56]. Nanocellulose-based coatings usually have smooth surfaces and low porosity due to their densely packed structures. Corona pre-treatment increases the surface energy of nanocellulose coatings, and aids the adhesion with extrusion polymers. As can be observed in Figure 4h, the corona treatment alone might not be sufficient to ensure adhesion between nanocellulose and thermoplastics. Blending oh hyper-platy kaolin into CNF-M increases the surface roughness and surface energy of nanocellulose-coated paperboard. This improves adhesion at nanocellulose/thermoplastic interface as is evident in Figure 6d, which shows the peak force required to pull a tape from the surface of extrusion-coated multilayer paperboard. Adhesion at the nanocellulose/baseboard interface is stronger than at thermoplastic interface due cationic starch pre-coating [24]. Moreover, the peeled tape was observed for residue, and in most cases, the failure was at nanocellulose/thermoplastic interface. Another possible way to improve adhesion with thermoplastics is to have a separate thin layer of pigment coating on top of nanocellulose-coated paperboard. This preserves the nanocellulose structure and therefore its barrier properties, while improving the adhesion with thermoplastics. Future work will address this issue.

CONCLUSIONS

Nanocellulose is gaining interest as a preferable material of choice for sustainable barrier packaging. The current work gives a brief overview at understanding and addressing the challenges that arise during high-throughput roll-to-roll processing of nanocelluloses into barrier coatings. Several grades of CNFs (pure mechanically defibrillated, chemically or enzymatically- pretreated) and CNCs were characterized for their rheological properties. Nanocellulose suspensions have high yield stresses, and adding dispersants such as CMC/NaPA reduce the yield stress of CNFs, thereby making it easier to handle otherwise high-viscosity suspensions.

CMC addition also increases the water retention, which in turn can have a positive impact on coating quality. A new Casson-power-cross model was proposed to explain the viscosity behavior of CNFs across a wide shear-rate region, and Herchel-Bulkley model explains the viscosity behavior of CNCs. All the suspensions are thixotropic with CMC or NaPA addition slowing down the structure recovery, which in turn can lead to improved coating quality.

A slot-die applicator was used to uniformly coat different nanocellulose grades across a wide range of coating thicknesses and suspension solid contents onto a paperboard. Cationic starch primer coating was used to improve the adhesion at nanocellulose/paperboard interface. To protect nanocellulose from moisture, several biodegradable thermoplastics and water-based dispersions were coated on top of nanocellulose-coated paperboard using extrusion or reverse gravure coating methods. Water vapor permeance of multilayer paperboards remained lower than the control single-layer moisture-barrier materials. Multilayer coatings also helped close any defects in the nanocellulose layer, thereby improving the oxygen and grease barriers, with OP values similar (or in some cases lower) to those of pure nanocellulose films. Plasticizers such as glycerol and sorbitol further improve oxygen barrier of the multilayer paperboards, and kaolin addition improves the adhesion at nanocellulose/thermoplastic interface.

This work provides insight into understanding how yield stress, dispersant type and loading, thixotropy, and water release influence coatability of different grades of nanocelluloses during high-throughput coating processes. Moreover, the approach of processing nanocellulose and moisture barrier materials together into multilayer structures complements the shortcomings of each other and produces a paperboard with superior barrier properties that is both bio-based and biodegradable.

ACKNOWLEDGMENTS

The authors thanks the following persons and companies for their respective contributions.

Prof. Douglas Bousfield, University of Maine for CNF-M. Dr. Tiffany Abitbol and Dr. Christian Aulin, RISE – Research Institutes of Sweden for CNF-C and adhesion measurements. SAPPI, Netherlands for CNF-S. Prof. Julien Bras and Dr. Gabriel Banvillet, Université Grenoble Alps for CNF-E. Melodea Ltd. for CNC-M. Celluforce Inc. for CNC-C. CP-Kelco for CMC. BASF for NaPA. Imerys for Barrisurf HX. Chemigate for Cationic starch. Dr. Johanna Lahti and Prof. Jurkka Kuusipalo, Tampere University for extrusion coatings and oxygen barrier measurements. Luyao Wang for TEM. Diosángeles Soto Véliz for Grease barrier characterization. Dr. Vinay Kumar, Aayush Jaiswal, Himal Ghimire for help with slot-die coatings.

Funding sources: Åbo Akademi Graduate School of Chemical Engineering, Magnus Ehrnrooth foundation, Finnish Forest Products Engineers Association, and Walter Ahlström Foundation.

The authors declare no competing financial interest.

REFERENCES

[1] PlasticsEurope, "Plastics – the facts 2021," tech. rep., Plastics Europe, 2021.
[2] J. Gaffey, H. McMahon, E. Marsh, K. Vehmas, T. Kymäläinen, and J. Vos, "Understanding consumer perspectives of bio-based products—a comparative case study from Ireland and The Netherlands," *Sustainability*, vol. 13, no. 11, 2021.
[3] I. Delioglamnis, E. Kouzi, E. Tsagaraki, M. Bougiouklis, and I. Tollias, "D2.4 public perception of bio-based products – societal needs and concerns," tech. rep., BIOWAYS Deliverable D2.4, 2018.
[4] E. Commission and D.-G. for Communication, *Circular Economy Action Plan: For a Cleaner and More Competitive Europe*. Publications Office, 2020.
[5] T. Abitbol, A. Rivkin, Y. Cao, Y. Nevo, E. Abraham, T. Ben-Shalom, S. Lapidot, and O. Shoseyov, "Nanocellulose, a tiny fiber with huge applications," *Current Opinion in Biotechnology*, vol. 39, pp. 76–88, 2016.
[6] B. Thomas, M. C. Raj, J. Joy, A. Moores, G. L. Drisko, and C. Sanchez, "Nanocellulose, a versatile green platform: from biosources to materials and their applications," *Chemical Reviews*, vol. 118, no. 24, pp. 11575–11625, 2018.
[7] S. S. Ahankari, A. R. Subhedar, S. S. Bhadauria, and A. Dufresne, "Nanocellulose in food packaging: A review," *Carbohydrate Polymers*, vol. 255, p. 117479, 2021.
[8] M. A. Hubbe, A. Ferrer, P. Tyagi, Y. Yin, C. Salas, L. Pal, and O. J. Rojas, "Nanocellulose in thin films, coatings, and plies for packaging applications: A review," *BioResources*, vol. 12, no. 1, pp. 2143–2233, 2017.
[9] FutureMarkets, "The nanocellulose market, production and pricing report 2021," tech. rep., Future Markets Inc., 2021.
[10] I. Siró and D. Plackett, "Microfibrillated cellulose and new nanocomposite materials: a review," *Cellulose*, vol. 17, no. 3, pp. 459–494, 2010.
[11] A. Isogai, T. Saito, and H. Fukuzumi, "Tempo-oxidized cellulose nanofibers," *Nanoscale*, vol. 3, no. 1, pp. 71–85, 2011.
[12] H. Liimatainen, M. Visanko, J. A. Sirviö, O. E. Hormi, and J. Niinimaki, "Enhancement of the nanofibrillation of wood cellulose through sequential periodate–chlorite oxidation," *Biomacromolecules*, vol. 13, no. 5, pp. 1592–1597, 2012.
[13] A. Naderi, T. Lindström, J. Sundström, T. Pettersson, G. Flodberg, and J. Erlandsson, "Microfluidized carboxymethyl cellulose modified pulp: a nanofibrillated cellulose system with some attractive properties," *Cellulose*, vol. 22, no. 2, pp. 1159–1173, 2015.
[14] M. Ghanadpour, F. Carosio, P. T. Larsson, and L. Wågberg, "Phosphorylated cellulose nanofibrils: a renewable nanomaterial for the preparation of intrinsically flame-retardant materials," *Biomacromolecules*, vol. 16, no. 10, pp. 3399–3410, 2015.

[15] M. Pääkkö, M. Ankerfors, H. Kosonen, A. Nykänen, S. Ahola, M. Österberg, J. Ruokolainen, J. Laine, P. T. Larsson, O. Ikkala, *et al.*, "Enzymatic hydrolysis combined with mechanical shearing and high-pressure homogenization for nanoscale cellulose fibrils and strong gels," *Biomacromolecules*, vol. 8, no. 6, pp. 1934–1941, 2007.

[16] O. Nechyporchuk, M. N. Belgacem, and J. Bras, "Production of cellulose nanofibrils: A review of recent advances," *Industrial Crops and Products*, vol. 93, pp. 2–25, 2016.

[17] M. Mariano, N. El Kissi, and A. Dufresne, "Cellulose nanocrystals and related nanocomposites: Review of some properties and challenges," *Journal of Polymer Science Part B: Polymer Physics*, vol. 52, no. 12, pp. 791–806, 2014.

[18] J. D. P. de Amorim, K. C. de Souza, C. R. Duarte, I. da Silva Duarte, F. d. A. S. Ribeiro, G. S. Silva, P. M. A. de Farias, A. Stingl, A. F. S. Costa, G. M. Vinhas, *et al.*, "Plant and bacterial nanocellulose: Production, properties and applications in medicine, food, cosmetics, electronics and engineering. a review," *Environmental Chemistry Letters*, vol. 18, no. 3, pp. 851–869, 2020.

[19] Q. Wang, Q. Yao, J. Liu, J. Sun, Q. Zhu, and H. Chen, "Processing nanocellulose to bulk materials: A review," *Cellulose*, vol. 26, no. 13, pp. 7585–7617, 2019.

[20] V. Kumar, B. Nazari, D. Bousfield, and M. Toivakka, "Rheology of microfibrillated cellulose suspensions in pressure-driven flow," *Applied Rheology*, vol. 26, no. 4, pp. 24–34, 2016.

[21] A. I. Koponen, "The effect of consistency on the shear rheology of aqueous suspensions of cellulose micro-and nanofibrils: a review," *Cellulose*, vol. 27, no. 4, pp. 1879–1897, 2020.

[22] M. A. Hubbe, P. Tayeb, M. Joyce, P. Tyagi, M. Kehoe, K. Dimic-Misic, and L. Pal, "Rheology of nanocellulose-rich aqueous suspensions: a review," *BioResources*, vol. 12, no. 4, pp. 9556–9661, 2017.

[23] V. Kumar, A. Elfving, H. Koivula, D. Bousfield, and M. Toivakka, "Roll-to-roll processed cellulose nanofiber coatings," *Industrial & Engineering Chemistry Research*, vol. 55, no. 12, pp. 3603–3613, 2016.

[24] R. Koppolu, T. Abitbol, V. Kumar, A. K. Jaiswal, A. Swerin, and M. Toivakka, "Continuous roll-to-roll coating of cellulose nanocrystals onto paperboard," *Cellulose*, vol. 25, no. 10, pp. 6055–6069, 2018.

[25] R. Koppolu, J. Lahti, T. Abitbol, A. Swerin, J. Kuusipalo, and M. Toivakka, "Continuous processing of nanocellulose and polylactic acid into multilayer barrier coatings," *ACS Applied Materials & Interfaces*, vol. 11, no. 12, pp. 11920–11927, 2019.

[26] R. A. Chowdhury, C. Clarkson, and J. Youngblood, "Continuous roll-to-roll fabrication of transparent cellulose nanocrystal (CNC) coatings with controlled anisotropy," *Cellulose*, vol. 25, no. 3, pp. 1769–1781, 2018.

[27] D. Beneventi, E. Zeno, and D. Chaussy, "Rapid nanopaper production by spray deposition of concentrated microfibrillated cellulose slurries," *Industrial Crops and Products*, vol. 72, pp. 200–205, 2015. Special issue derived from International Conference on Bio-based Materials and Composites.

[28] K. L. Spence, R. A. Venditti, O. J. Rojas, Y. Habibi, and J. J. Pawlak, "A comparative study of energy consumption and physical properties of microfibrillated cellulose

produced by different processing methods," *Cellulose*, vol. 18, no. 4, pp. 1097–1111, 2011.

[29] P. Tyagi, K. S. Salem, M. A. Hubbe, and L. Pal, "Advances in barrier coatings and film technologies for achieving sustainable packaging of food products–a review," *Trends in Food Science & Technology*, vol. 115, pp. 461–485, 2021.

[30] L. Dai, Z. Long, J. Chen, X. An, D. Cheng, A. Khan, and Y. Ni, "Robust guar gum/cellulose nanofibrils multilayer films with good barrier properties," *ACS Applied Materials & Interfaces*, vol. 9, no. 6, pp. 5477–5485, 2017.

[31] C. Aulin, E. Karabulut, A. Tran, L. Wågberg, and T. Lindström, "Transparent nanocellulosic multilayer thin films on polylactic acid with tunable gas barrier properties," *ACS applied materials & interfaces*, vol. 5, no. 15, pp. 7352–7359, 2013.

[32] C. Aulin and G. Strö, "Multilayered alkyd resin/nanocellulose coatings for use in renewable packaging solutions with a high level of moisture resistance," *Industrial & Engineering Chemistry Research*, vol. 52, no. 7, pp. 2582–2589, 2013.

[33] J. Vartiainen, Y. Shen, T. Kaljunen, T. Malm, M. Vähä-Nissi, M. Putkonen, and A. Harlin, "Bio-based multilayer barrier films by extrusion, dispersion coating and atomic layer deposition," *Journal of Applied Polymer Science*, vol. 133, no. 2, 2016.

[34] S. Spoljaric, A. Salminen, N. Dang Luong, P. Lahtinen, J. Vartiainen, T. Tammelin, and J. Seppälä, "Nanofibrillated cellulose, poly (vinyl alcohol), montmorillonite clay hybrid nanocomposites with superior barrier and thermomechanical properties," *Polymer composites*, vol. 35, no. 6, pp. 1117–1131, 2014.

[35] A. Cherpinski, S. Torres-Giner, J. Vartiainen, M. S. Peresin, P. Lahtinen, and J. M. Lagaron, "Improving the water resistance of nanocellulose-based films with polyhydroxyalkanoates processed by the electrospinning coating technique," *Cellulose*, vol. 25, no. 2, pp. 1291–1307, 2018.

[36] E.-L. Hult, M. Iotti, and M. Lenes, "Efficient approach to high barrier packaging using microfibrillar cellulose and shellac," *Cellulose*, vol. 17, no. 3, pp. 575–586, 2010.

[37] B. Bideau, J. Bras, N. Adoui, E. Loranger, and C. Daneault, "Polypyrrole/nanocellulose composite for food preservation: barrier and antioxidant characterization," *Food packaging and shelf life*, vol. 12, pp. 1–8, 2017.

[38] C. C. Satam, C. W. Irvin, A. W. Lang, J. C. R. Jallorina, M. L. Shofner, J. R. Reynolds, and J. C. Meredith, "Spray-coated multilayer cellulose nanocrystal—chitin nanofiber films for barrier applications," *ACS Sustainable Chemistry & Engineering*, vol. 6, no. 8, pp. 10637– 10644, 2018.

[39] A. Naderi, T. Lindström, J. Sundström, G. Flodberg, and J. Erlandsson, "A comparative study of the properties of three nanofibrillated cellulose systems that have been produced at about the same energy consumption levels in the mechanical delamination step," *Nordic Pulp & Paper Research Journal*, vol. 31, no. 3, pp. 364–371, 2016.

[40] A. Naderi, T. Lindström, and J. Sundström, "Carboxymethylated nanofibrillated cellulose: rheological studies," *Cellulose*, vol. 21, no. 3, pp. 1561–1571, 2014.

[41] A. K. Jaiswal, V. Kumar, A. Khakalo, P. Lahtinen, K. Solin, J. Pere, and M. Toivakka, "Rheological behavior of high consistency enzymatically fibrillated cellulose suspensions," *Cellulose*, vol. 28, no. 4, pp. 2087–2104, 2021.

[42] M.-C. Li, Q. Wu, R. J. Moon, M. A. Hubbe, and M. J. Bortner, "Rheological aspects of cellulose nanomaterials: Governing factors and emerging applications," *Advanced Materials*, vol. 33, no. 21, p. 2006052, 2021.

[43] T. Mezger, *The Rheology Handbook: 4th Edition*. European Coatings Tech Files, Vincentz Network, 2011.

[44] V. Kumar, V. R. Koppolu, D. Bousfield, and M. Toivakka, "Substrate role in coating of microfibrillated cellulose suspensions," *Cellulose*, vol. 24, no. 3, pp. 1247–1260, 2017.

[45] P. Miettinen, S. Auvinen, J. Kuusipalo, and S. Haakana, "Validity of traditional barriertesting methods to predict the achievable benefits of the new generation water based barrier coatings for packaging materials," in *PTS Coating Symposium*, pp. 328–342, 2015.

[46] V. Arantes, I. K. Dias, G. L. Berto, B. Pereira, B. S. Marotti, and C. F. Nogueira, "The current status of the enzyme-mediated isolation and functionalization of nanocelluloses: production, properties, techno-economics, and opportunities," *Cellulose*, pp. 1–60, 2020.

[47] G. Banvillet, E. Gatt, N. Belgacem, and J. Bras, "Cellulose fibers deconstruction by twinscrew extrusion with in situ enzymatic hydrolysis via bioextrusion," *Bioresource Technology*, vol. 327, p. 124819, 2021.

[48] F. P. A. Kutty, R. Koppolu, A. Swerin, F. Lundell, and M. Toivakka, "Numerical analysis of slot die coating of nanocellulosic materials," *TAPPI Journal*, vol. 19, no. 11, pp. 575–582, 2020.

[49] G. Drage, O. Tammn, and J. Husband, "Pigments," in *Pigment coating and surface sizing of paper* (J. Paltakari, ed.), vol. 11, pp. 72–190, Paper Engineers' Association/ Paperi ja Puu Oy, 2 ed., 2009.

[50] A. Karppinen, *Rheology and flocculation of polymer-modified microfibrillated cellulose suspensions*. Doctoral thesis, Aalto university, School of Chemical Technology, 2014.

[51] M. Singhvi and D. Gokhale, "Biomass to biodegradable polymer (pla)," *RSC advances*, vol. 3, no. 33, pp. 13558–13568, 2013.

[52] S. Rafiqah, A. Khalina, A. S. Harmaen, I. A. Tawakkal, K. Zaman, M. Asim, M. Nurrazi, and C. H. Lee, "A review on properties and application of bio-based poly (butylene succinate)," *Polymers*, vol. 13, no. 9, p. 1436, 2021.

[53] K. W. Meereboer, M. Misra, and A. K. Mohanty, "Review of recent advances in the biodegradability of polyhydroxyalkanoate (pha) bioplastics and their composites," *Green Chemistry*, vol. 22, no. 17, pp. 5519–5558, 2020.

[54] U. Witt, T. Einig, M. Yamamoto, I. Kleeberg, W.-D. Deckwer, and R.-J. Müller, "Biodegradation of aliphatic–aromatic copolyesters: evaluation of the final biodegradability and ecotoxicological impact of degradation intermediates," *Chemosphere*, vol. 44, no. 2, pp. 289–299, 2001.

[55] F. Wu, M. Misra, and A. K. Mohanty, "Challenges and new opportunities on barrier performance of biodegradable polymers for sustainable packaging," *Progress in Polymer Science*, vol. 117, p. 101395, 2021.

[56] J. Kuusipalo and A. Savolainen, "Adhesion phenomena in (co) extrusion coating of paper and paperboard," *Journal of adhesion science and technology*, vol. 11, no. 8, pp. 1119– 1135, 1997.

HIGH-THROUGHPUT PROCESSING OF NANOCELLULOSES INTO BIODEGRADABLE BARRIER COATINGS

Rajesh Koppolu and Martti Toivakka

Laboratory of Natural Materials Technology, Åbo Akademi University, 20500 Turku, Finland

Jee-Hong Lee Seoul National University

It is really interesting to see this scaling up and moving one step closer to commercial applications of this fabulous nanomaterial: nanocelluloses. My question is that, can you make some comments in terms of the runnability? Because when I saw the slides 14, 15, I mean the video, I have seen some kind of clusters on the edges of the coatings and also it seems that the coating speed is a little bit slow, so how to make improvements on points like that?

Rajesh Koppolu

Yes. So first, the clusters that you saw, they are outside the coating head. So, like I said, this is a pressure driven flow, and we have metering at the bottom, but sometimes something has come up, but not in the coating area, it is from the sides. So, that is what we saw. and if we do full width coating, then probably they would stay outside the paper's area. The speed is quite low, because the solid content is less and the dryers were added as we went on, but if you build a machine from the start or have proper drying control, then it should be much better. And the highest speed we went was 10 metres per minute.

Discussion

Janet Preston Imerys Minerals Ltd

What do you think are the big hurdles to overcome before this nanocellulose coating becomes a reality and you find packaging actually being made with these interesting layer structures?

Rajesh Koppolu

I think one of the biggest hurdles is still the solid contents of the suspensions are quite low and it gets more and more challenging to coat as we go to higher solids content, and it gets very expensive if you want to dry just a 2 or 3% suspension. So that would be one of the bigger challenges, at least that I would think of. There are now enzymatically pre-treated nanocellulose and there are new grades coming up whose solid contents are going up. Now there are grades at 10%, 15% solid content already, so that would be interesting to see if they give any similar properties.

Alexander Bismarck University of Vienna

You promised to get rid of multilayer coatings and in the end, you had to produce multilayer coatings. The delamination of the polymer layer is due to the fact that you coat the polymer from the melt and then you have massive shrinkage during cooldown and crystallisation, which does not fit the thermal expansion of your paper composite?

Rajesh Koppolu

Yeah, I think it is something like that. So, it is maybe both the layers are incompatible with the shrinkage. So that is why when we have the Kaolin added into the nanocellulose, I think it is creating some kind of micro roughness on the top, because I looked at the orientation of the kaolin pigments on the surface which can be determined by FTIR measurements. The orientation depends on which way the OH groups are pointing and it showed that it is a random arrangement. Because the viscosity of suspension is so high that maybe the clay particles would not arrange or would not be flat, so maybe that is creating some roughness on the top, which then stops the thermoplastic from shrinking or delaminating.

Ramesh Natarajan Westrock – Richmond VA

I was just wondering about the safety because there are a lot of articles on nanocellulose and possible safety issues, so what is your comment and what are we supposed to do?

Rajesh Koppolu

I do not have any comment with this. There are some studies that say it is safe. Some say, well, they need to still look at it. But I think it is an evolving field and I am not an expert in looking at safety, but if it is safe then it is a good material to use. Of course, it has its challenges.

Bill Sampson University of Manchester

For as long as people have beaten fibres to make paper, they have been creating nanocellulose. To the best of my knowledge, it has been quite safe for 2,000 years.

Torbjorn Wahlstrom Stora Enso

Bill, that is right. But it does not really matter if the regulations say something else. I am not into that area, but it is something that we do need to take seriously and handle, otherwise there will be no products with those new materials.